Multicarrier Reflectometry

Suketu Naik, Cynthia M. Furse, *Senior Member, IEEE*, and Behrouz Farhang-Boroujeny, *Senior Member, IEEE*

***Abstract*—A new reflectometry method called multicarrier reflectometry (MCR) for fault location in cables is proposed. MCR combines a weighted set of sinusoidal excitations into a signal that is sent down the wire. The reflected signal from the cable under test is analyzed in order to determine the length of the wire or possible location of a fault. In the frequency domain, the phase response of the reflected signal contains the desired information. This method provides a system with greater flexibility than conventional frequency domain reflectometry, better noise immunity than time domain reflectometry, and the ability to employ frequency agility to avoid certain interference bands. This method introduces an approach to the generation of test signals that allows more control over the bandwidth of the test signal. All the data analysis can be done in the digital domain after the reflected wave is sampled, thus enabling the use of more meticulous digital signal processing techniques. The major advantage of this method is the potential use in live cables carrying other signals such as power or data. The bandwidth over which the test signals are transmitted can be chosen specifically to avoid the bandwidth of the live wire signal.**

***Index Terms*—Fault location, reflectometry, wiring.**

I. Introduction

IN AN aging aircraft, the condition of the wires and cables should be thoroughly and regularly inspected to avoid any problems. However, this is difficult and often impossible today. A short circuit, broken wire, or a fray can lead to an in-flight fire or other disastrous situation [1]. Automated electronic techniques such as the one that will be described in this paper are very much desired for this application. In particular, methods to locate small faults before they create system level problems are desired. These faults leave impedance discontinuities that are too small to detect with any of today's reflectometry methods. Methods that can locate the fault when its impedance discontinuity is larger, such as when water drips on a crack in the wire or when the wire vibrates against a metal structure have more promise of locating these anomalies. This requires being able to test the wires continuously while they are live and in flight, which requires a new class of reflectometry methods.

Several techniques and methods have been used successfully to locate faults on wiring. Some of these methods include time domain reflectometry (TDR) [2] phase detection frequency domain reflectometry (PD-FDR) [3], mixed-signal reflectometry (MSR) [4], and capacitance measurement [5], [18] for dead (not powered) wires. On the other hand, spread spectrum time domain reflectometry (SSTDR) and sequence time domain reflectometry (STDR) have been shown to be feasible for use on live wires [6], [16].

The techniques mentioned above have been very successful for locating wiring faults. In PD-FDR [3], a set of stepped frequency sine waves is sent down the cable. Then the reflected wave is separated from the incident wave using directional couplers and mixed (multiplied) with the incident wave to produce a DC voltage (proportional to phase shift) that varies sinusoidally as the frequency is swept linearly. The DC function that is produced is sinusoidal, and the number of periods in the function is proportional to the length of the cable. MSR utilizes a similar concept but does not require directional couplers [4].

Multiple carrier reflectometry (MCR) is analytically similar to PD-FDR and MSR in the sense that it also uses multifrequency test signals. It is very different in practice, however. While PD-FDR and MSR utilize one frequency at a time, MCR combines all the frequencies in one periodic test signal. In other words, while PD-FDR and MSR follow a sequential testing mode, MCR effectively operates in a parallel testing mode. Thus, it can complete a measurement in a much shorter time, hopefully on a live wire while the fault is present. MCR also has some similarities to TDR. The step function that TDR transmits represents the limit where MCR uses an infinite band of simultaneous frequencies with phases aligned. Of course, such a system is not physically realizable.

The way MCR handles the signals leads to greater flexibility than PD-FDR and MSR systems, wider dynamic frequency agility, more control over the bandwidth of the test signal, deployment of sophisticated signal processing techniques, and implementation on digital hardware platforms such as digital signal processors (DSP), field programmable gate arrays (FPGA), and application-specific integrated circuits (ASIC). The most important feature of this method is its flexibility to test live wires. The bandwidth over which the test signal is transmitted can be chosen to avoid the bandwidth of the live wire signals (power or data). The reason that testing live wires is so important is that all reflectometry methods are limited by the magnitude of the reflection they can detect returning from a fault. Open and short circuits return all of the power (in and out of phase, respectively) and are, therefore, the easiest to detect. An impedance-matched load returns no power and is, therefore, impossible to detect. Small anomalies on the wire (insulation damage and even some conductor damage) produces reflections that are far too small to detect (generally less than 1%) [15], [19]. If, instead, the system can be used when the wire is live, an intermittent condition that caused a small-duration near-short or near-open condition could be detected.

Manuscript received January 12, 2005; revised March 11, 2005. The associate editor coordinating the review of this paper and approving it for publication was Prof. Eugenii Katz.

S. Naik is with the Spawar Systems Center, San Diego CA 92152-5001 USA (e-mail: suketu@spawar.navy.mil).

C. M. Furse is with the Department of Electrical and Computer Engineering, University of Utah, Salt Lake City, UT 84112 USA, and also with the LiveWire Test Labs, Inc., Salt Lake City, UT 84117 USA (e-mail: cfurse@ece.utah.edu).

B. Farhang-Boroujeny is with the Department of Electrical and Computer Engineering, University of Utah, Salt Lake City, UT 84112 USA (e-mail: farhang@ece.utah.edu).

Digital Object Identifier 10.1109/JSEN.2006.874018

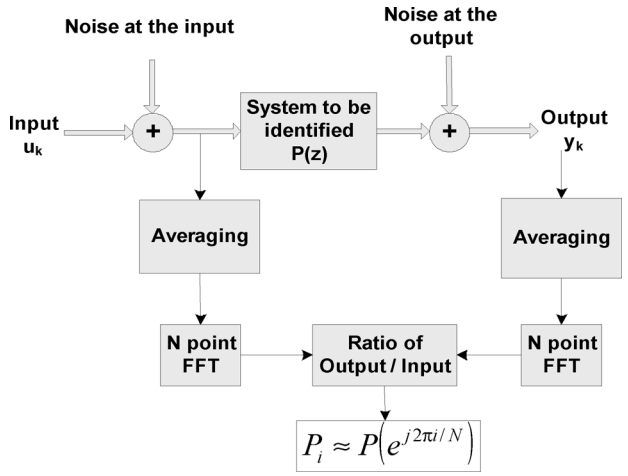

Fig. 1. Block diagram of system identification method from [7].

This paper is organized as follows. Section II provides the basic theory behind MCR. Section III discusses the general setup of MCR. Section IV expounds on the modeling of the MCR signals and the optimization technique to analyze the observed data. Experimental setup of MCR is described and the corresponding results are presented in Section V. Live wire simulations are shown in Section VI. Section VII summarizes the paper and draws important conclusions.

Throughout this paper, the following notations are used. Lowercase bold letters are used for vectors. Uppercase bold letters are used to denote matrices. Scalar variables are denoted by nonbold letters. The superscripts T and H denote transpose and Hermitian, respectively.

II. Basic Theory of MCR

MCR is based on a system identification technique [7]. In [7], an excitation signal which is the summation of a number of harmonically related sine waves is used to identify an unknown plant. In particular, the excitation signal u_k (in the discrete-time domain) is chosen as

$$u_k = \sum_{i=0}^{N/2} c_i \sin\left(\frac{2\pi i}{N}k + \theta_i\right) \tag{1}$$

where the phases θ_i of the sine waves comprising the test signal are chosen with the goal of minimizing the peak to root mean power of u_k, c_i are the magnitudes of the sine waves, and N is the number of samples in the signal, and k denotes the sample index.

There are two characteristics of u_k that should be noted: 1) u_k is periodic and has the period N. 2) The coefficients c_i can differ. In particular, they can be zero for a band that contains an existing signal on the wire that we wish to avoid. When u_k is applied to a plant $P(z)$, as shown in Fig. 1, the associated output y_k is also periodic and has the same period N. If the plant is free of noise and any signals other than u_k, the sample-wise division of the discrete Fourier transforms (DFT) of one period of y_k and u_k at the frequency samples which have nonzero excitation, gives the frequency response of the plant at those frequencies. Thus, the unknown plant is identified in the frequency domain. A conversion from the frequency domain to the time domain can subsequently be performed if the time domain response of the plant is desired [7]. When the input and output are contaminated by additional signals (other than u_k and y_k, respectively), the signals at the plant input and output may be averaged over a number of periods before performing DFTs. Averaging suppresses the undesirable signals and results in a more accurate estimate of the plant response. Fig. 1 summarizes the above method in a schematic form. The DFTs are performed using fast Fourier transforms (FFT). The final result of the measurement is an estimate of the plant frequency response at the points of excitations. This is denoted by

$$P_i \approx P(e^{j2\pi i/N}). \tag{2}$$

A. Time Delay and Cable Model

A simple delay model with transfer function $P(z) = z^{-\tau}$ can be used to simulate the cable and replace the system in Fig. 1. By efficiently calculating the time delay produced by the system, i.e., a cable, we can estimate the length (distance or length = time delay $\times$ velocity of propagation) [8]. The time delay τ is computed by estimating the group delay exhibited by the system at the frequencies present in the output signal. Group delay is a measure of the average delay of the system as a function of frequency. It is defined as the negative of the first derivative of the system phase response.

Therefore, the group delay (seconds) is defined as

$$\tau = -\partial\phi/\partial\omega \tag{3}$$

where ϕ is the phase response of the system in radians, and ω is the angular frequency in radians per second. We also define the normalized time delay

$$\tau_D = \tau/T_s \tag{4}$$

where T_s is the sampling period (seconds).

III. MCR Setup

A typical MCR setup is shown in Fig. 2. The idea is to use an FPGA board that contains a digital to analog converter (D/A) and an analog to digital converter (A/D) channels in order to transmit and receive the test signals, respectively. This board can be interfaced with a PC in order to download and analyze the data acquired by the FPGA. The setup shown in Fig. 2 creates an undesirable and unavoidable branching or network of cables at the T-junction.

A BNC T-junction connector must be used as shown in Fig. 2 in order to make the necessary connections. Fig. 3 shows the network created by such connections in detail for a 50-Ω cable. One end of the connector is attached to the D/A of the board. The other end is connected to the A/D of the board, and the third end

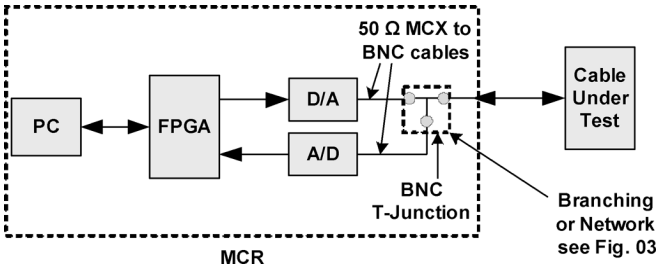

Fig. 2. MCR setup.

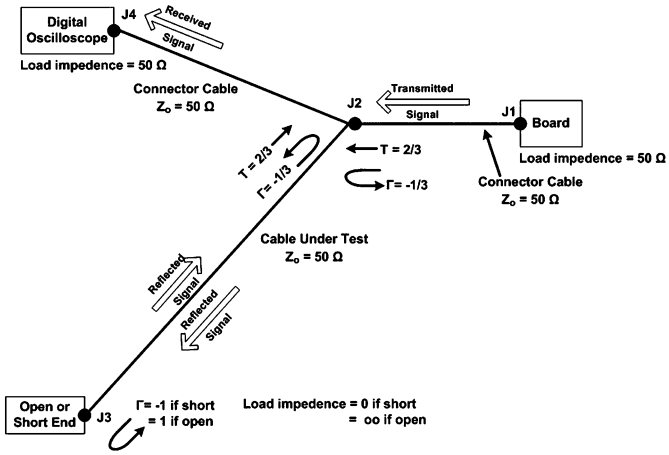

Fig. 3. MCR test setup and resultant creation of a network.

is connected to the cable under test. As shown in Fig. 3, there are no reflections at junctions J1 and J4, which act as the input and output ports of this test system since the load impedances at these junctions are matched to 50 Ω. Hence, the only reflections that occur are due to the cables. Also, the characteristic impedances of the cables determine the reflection coefficient and transmission coefficient values shown in Fig. 3. These values scale the amplitudes of the transmitted and reflected signals at junctions J2 and J3, respectively. The reflections show up with the time delay exhibited by the cables. Because time is equal to distance divided by the velocity of propagation, the length of the cable and the time delay exhibited by the cable are directly proportional. A detailed analysis of this network is presented in [8].

IV. Modeling and Optimization Technique

The signal received by the A/D in Fig. 3 can be described as

$$r_s(t) = \alpha_o x(t) + \alpha_1 x(t-2\tau) + \alpha_2 x(t-4\tau) + \dots \quad (5)$$

where $r_s(t)$ is the received signal, $x(t)$ is the transmitted signal, α_o,α_1, and α_2 are the coefficients that denote changes in the amplitude due to the transmission coefficient T and reflection coefficient Γ as shown in Fig. 3, and τ is the time delay proportional to the length of the cable L divided by the velocity of propagation.

Taking the Fourier transform of both the sides of (5), we obtain

$$R_s(\omega) = \alpha_0 X(\omega) + \alpha_1 X(\omega) e^{-j\omega(2\tau)} + \alpha_2 X(\omega) e^{-j\omega(4\tau)}. \quad (6)$$

From (6), the transfer function of the system setup in Fig. 3 is obtained as

$$P(\omega) = \frac{R_s(\omega)}{X(\omega)} = \alpha_0 + \alpha_1 e^{-j\omega(2\tau)} + \alpha_2 e^{-j\omega(4\tau)}. \quad (7)$$

Through the procedure and test signal that were introduced in Section II, one can obtain the values of $P(\omega)$ at the excitation frequencies. The parameters α_o, α_1, α_2, and τ are subsequently optimized to match the measured response $P(\omega)$. An estimate of these parameters can be obtained when there are at least four excitation frequencies. The presence of more excitation frequencies allows a more accurate estimate of the parameters as explained below.

Taking into account the measurement noise $\mathbf{n}$, define the column vector of the sampled transfer function

$$\hat{\mathbf{p}} = \mathbf{p} + \mathbf{n} \quad (8)$$

where $\mathbf{p} = [P(\omega_1)\ P(\omega_2) \cdots P(\omega_M)]^T$ is the vector of the values $P(\omega)$ at the excited frequencies (called $\omega_1, \omega_2 \cdots, \omega_M$) and $\mathbf{n}$ is the vector of the measurement noise samples. Defining the normalized frequencies $\Omega_i = \omega_i T_s$ and recalling (4), from (7), we obtain

$$\mathbf{p} = \begin{bmatrix} 1 & e^{-j2\Omega_1\tau_D} & e^{-j4\Omega_1\tau_D} \\ 1 & e^{-j2\Omega_2\tau_D} & e^{-j4\Omega_2\tau_D} \\ \vdots & \vdots & \vdots \\ 1 & e^{-j2\Omega_M\tau_D} & e^{-j4\Omega_M\tau_D} \end{bmatrix} \begin{bmatrix} \alpha_0 \\ \alpha_1 \\ \alpha_2 \end{bmatrix}. \quad (9)$$

In the least-squares optimization, the goal is to minimize the sum of squares of the elements of the error vector $\mathbf{e} = \mathbf{p} - \hat{\mathbf{p}}$ [9]. Mathematically, this is formed by defining cost function

$$\psi = \mathbf{e}^H \mathbf{e} \quad (10)$$

(where $\mathbf{e}^{\mathrm{H}}$ is the Hermitian of $\mathbf{e}$) and finding the parameters α_o, α_1, α_2 and τ_D that minimize ψ.

The cost function ψ is quadratic with the parameters α_o, α_1, α_2, and, thus, for a given τ_D, it has a single minimum that can be obtained as explained below. However, in terms of τ_D, the form ψ is nontrivial and would exhibit a multimodal form. We deal with this nontrivial relationship of τ_D and ψ, as follows. We choose τ_D from a dense grid of values within the expected range and minimize ψ with respect to α_o, α_1, and α_2. The smallest value of ψ among these minimized values is the desired least squares solution, and the corresponding τ_D is the desired time delay from which the line length L is obtained.

Let

$$\mathbf{X} = \begin{bmatrix} 1 & e^{-j2\Omega_1\tau_D} & e^{-j4\Omega_1\tau_D} \\ 1 & e^{-j2\Omega_2\tau_D} & e^{-j4\Omega_2\tau_D} \\ \vdots & \vdots & \vdots \\ 1 & e^{-j2\Omega_M\tau_D} & e^{-j4\Omega_M\tau_D} \end{bmatrix} \text{ and } \mathbf{a} = \begin{bmatrix} \alpha_0 \\ \alpha_1 \\ \alpha_2 \end{bmatrix}.$$

Using the above and substituting (9) in (10), we obtain

$$\psi = \hat{\mathbf{p}}^H \hat{\mathbf{p}} - 2\mathbf{a}^H \mathbf{X}^H \hat{\mathbf{p}} + \mathbf{a}^H \mathbf{X}^H \mathbf{X} \mathbf{a}. \quad (11)$$

Assuming that τ_D and, hence, $\mathbf{X}$ is fixed, setting the gradient of ψ with respect to $\mathbf{a}$ to zero leads to the optimized solution

$$\mathbf{a_{opt}} = [\mathbf{X^H X}]^{-1}[\mathbf{X^H}\hat{\mathbf{p}}]. \tag{12}$$

After substituting this in (11), the minimum of ψ is found as

$$\psi_{\min} = \hat{\mathbf{p}}^H\hat{\mathbf{p}} - \mathbf{a}^H\mathbf{X}^H\hat{\mathbf{p}}. \tag{13}$$

V. Experimental Setup and Results

A. Experimental Setup

The implementation of the MCR requires five specific tasks:

1) generation of the desired signal in hardware;
2) transmission of this signal onto the cable under test;
3) sampling of the reflected signal;
4) carrying out the frequency domain analysis and, thus, estimating the time delay τ;
5) computing the length of the cable (distance to the fault) based on the estimated τ.

These tasks can be accomplished by exploring different combinations of hardware/software configurations. This section describes the particular configuration that was most fruitful in our experimental setup [8].

For the purposes of the research presented in this paper, it was desired to implement the fault location hardware in a digital signal processing (DSP) oriented FPGA device. Xilinx's DSP development board, Xtreme DSP Kit, was chosen. This development board includes two A/Ds with a 65 mega samples per second (MSPS) data rate and two D/As with 160 MSPS data rate [10]. The A/Ds and D/As are connected to the Xilinx Virtex-II FPGA device through a motherboard to form an efficient DSP board. The programming of the board is automated through a system-level design software called System Generator. With the aid of very high level design software such as System Generator and easy-to-use, well-integrated design flow, this board makes an excellent choice for fast and efficient transition from algorithm concept to hardware verification and allows a suitable debugging opportunity when a certain system model fails.

Due to an inherent conflict between the clock of the A/D or D/A and system model clock, the data transferred to the system model by the board (and vice a versa) became highly noisy and deformed (through both D/A and A/D). Therefore, a digital oscilloscope (Agilent 54 833A) with a sampling rate of 1 Giga samples per second was substituted for the data acquisition. A wideband coupler was used for the synchronization. This scheme is presented in Fig. 4.

The algorithm was partially implemented on the FPGA board. Partial implementation included the generation of the test data and conversion of these data into a continuous test signal. Fig. 5 shows an example of this test signal in the case where $\theta_i = 0$ and c_i is constant for all frequency components in (1). This is not an optimal test signal; however, its use is instructive for better visualization of the time delays (e.g., Fig. 7).

The sum of sinusoidal samples was generated and stored in a look up table in the FPGA. The content of this table, addressed

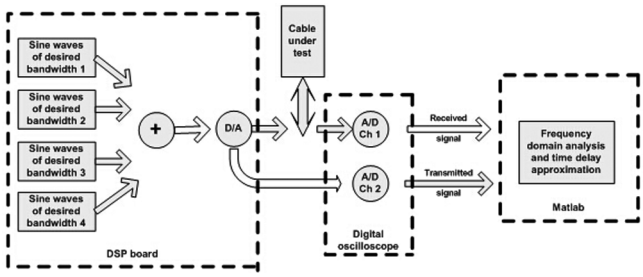

Fig. 4. Experimental setup for the implementation of the MCR.

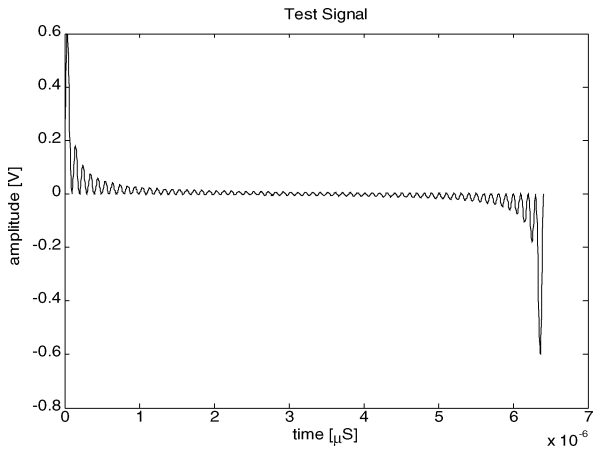

Fig. 5. Test signal: one period of the sum of sinusoids with $\theta = 0$ in (1).

by using an N-bit counter, was repeatedly sent to the cable under test through a D/A. The fundamental frequency of the generated periodic wave is

$$f_o = \frac{1}{T_s}\cdot\frac{1}{2^N} = \frac{f_s}{2^N} \tag{14}$$

where $f_s = 1/T_s$ is the rate of samples at the D/A output. $2^{\mathrm{N}} = 256$ was chosen, and a summation of $2^{\mathrm{N}}/4 = 64$ sinusoids was created, leaving a sufficient guard band for analog filtering and interpolation. This made $f_o = 156.25$ kHz. The amplitude of the sine waves was varied from -0.6 to $+0.6$ V. This amplitude range was chosen to provide a full two level transition for fixed-point arithmetic (e.g., rounding, truncation and saturation) used by the FPGA.

The major disadvantage of the type of test signal shown in Fig. 5 is that it contains impulsive samples at the beginning and end of the fundamental period. A periodic test signal for parameter estimation (e.g., finding frequency response or transfer function of a system) should have a low or minimum peak factor [7]. The peak factor of a signal is defined as the ratio of the difference of the maximum and the minimum value of the signal to its root-mean-square value [7]. The purpose of minimizing the peak factor is simply to maximize the signal power within the allowable amplitude range [11]. In other words, a minimum peak factor would distribute the energy of a wide-band signal over time [11]. For a given power spectrum, the peak factor of a periodic signal is also a function of the phase angles of the harmonics [12]. A minimum peak factor requires careful construction of the phase angles. For a signal

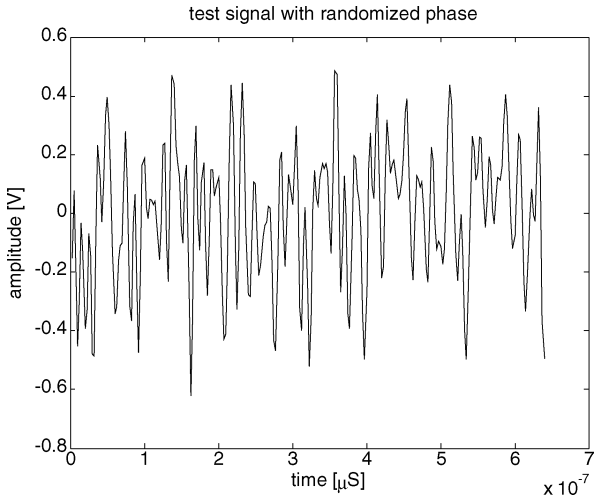

Fig. 6. Test signal: One period of the sum of sinusoids with randomized phase, i.e., no visible peak.

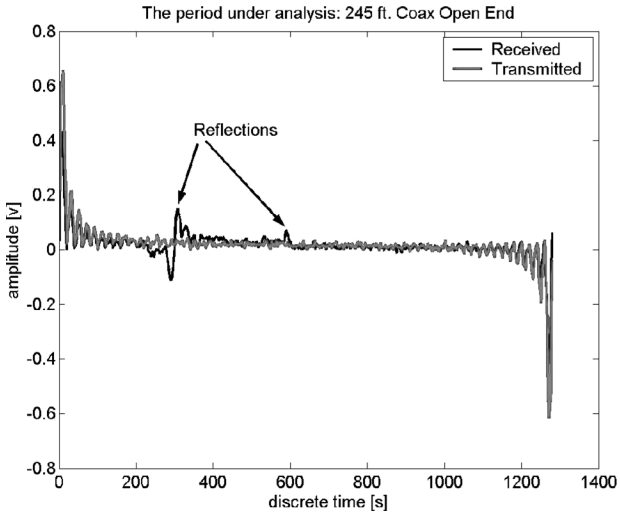

Fig. 7. Transmitted and received signals: 245-ft RG-58 coax with an open end.

with zero phase angle, such as the one shown in Fig. 5, the peak factor is generally large [12]. To minimize this peak factor further and to prevent impulsive transition, the sinusoids were summed up with randomized phase (using the "*rand*" function in Matlab). Hundreds of these different types of test signals were evaluated empirically to choose the test signal with the smallest peak factor, shown in Fig. 6; [11] and [12] contain additional information on other ways of reducing the peak factor. This signal has the appearance of pure noise, which has also been shown to be an effective test signal for fault location [13].

As shown in Fig. 4, the transmitted signal was stored in the digital oscilloscope. Then, a wideband -20-dB down coupler (not shown), was used to separate the received signal (on Channel 1) from the transmitted signal (on Channel 2). Then, Channel 2 was used to trigger Channel 1 in order to synchronize the transmitted signal and the received signal.

The major advantage of an implementation that uses digital logic is that it can offer faster switching among different output frequencies, fine frequency resolution, and operation over a broad spectrum of frequencies. Storing values in a look-up table is also FPGA area-efficient and draws little power. This gives us the ability to accurately produce and control waveforms of various frequencies. A sum of sinusoids with randomized phase was chosen as the test signal, because it has no single peak value and can, therefore, be effectively "hidden" within the noise and/or existing signal on the cable. This way of generating a desired test signal is also convenient for fast hopping speed in tuning the output frequency. Since the values of the sinusoids are controlled by linearly increasing modulo-N counter output values, the frequency can hop with virtually no overshoot or undershoot or analog-related loop settling-time anomalies often encountered in components such as the voltage controlled oscillator (VCO). Moreover, the digital architecture of this scheme eliminates the need for the manual tuning and tweaking related to component aging and temperature drift in analog frequency synthesizer solutions, such as a VCO.

B. Results

The test setup shown in Fig. 4 inadvertently created a branching or network of the cables as discussed earlier in Section III. All the cables used in the tests were RG58 coax with a characteristic impedance of roughly $Zo = 50\ \Omega$. It was concluded that the transmission coefficient (T) and reflection coefficient (Γ) values shown in Fig. 3 (calculated from Zo) scaled the reflected signals as shown in Fig. 7. Therefore, the received signal can be described as the addition of the scaled transmitted signal and the delayed versions of the transmitted signal (i.e., multiple reflections) as mentioned in Section IV. Fig. 7 shows the time domain versions of both the transmitted signal and the received signal as observed in this test for 245-ft long RG-58 cable with an open end. The test signal is a periodic pulse with positive and negative parts (i.e., a two level signal). As a result, the reflections also contain the dipole or two-level transitions as seen in Fig. 7.

When the test signal is constructed by randomizing phases of each of the sinusoids as mentioned earlier, the two-level transition is no longer present in the time-domain (see Fig. 6). The reflections caused by the cable are still present in the received signal and can be obtained in the frequency domain by the optimization technique as discussed in Section IV. A number of minima points are observed as seen in Fig. 8. It should be noted that these multiple minima are inherent in the optimization processing. Equation (7) has two terms, each of which can contribute to individual minima. The first minima in Fig. 8 occurs when τ is half of its optimal value. The global minima (the second in Fig. 8) will occur when τ is optimal, so that both terms in (7) match the channel model. The global minimum determines the delay τ and the line length. If the cable is branched, multiple sets of both the local and global minima will be observed. Methods to identify the branched cable topology should use both minima when determining where a reflection occurs. [17]

To obtain a better estimate of the global minimum, the optimization was rerun near the estimated minimum. This time, the optimization was concentrated on a few points around the

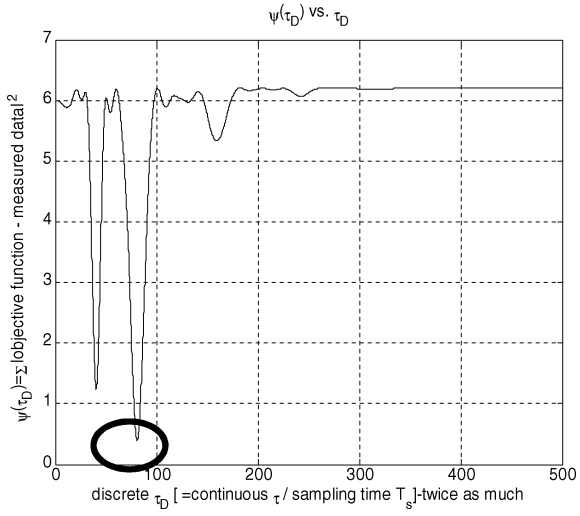

Fig. 8. Results of the optimization for 129.6833-ft RG-58 cable: Circle shows the location of the global minimum at 80.8 (see Fig. 9).

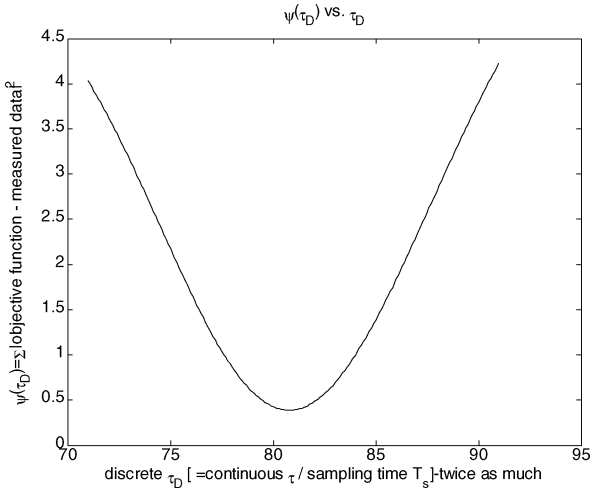

Fig. 9. Results of further optimization on various minima: Global minimum is found at 81.

global minimum, and the values of τ_{D} were changed in increments of 0.1. This resulted in a better global minimum as shown in Fig. 9. This method saves the complexity of the calculations and efficiently finds a global minimum when multiple minima are present. The results shown in Fig. 8 and 9 correspond to a 129-ft RG-58 coax cable. According to (8), the discrete-time delay exhibited by this cable would be 79 (twice as much), with the sampling frequency $f_s = 200$ MHz, and the velocity of propagation $V_p = 2 \times 10^8$ m/s. It should be noted that the accuracy of the measurements of this and any other reflectometry system will be limited by how well one knows the velocity of propagation of the cable, and how consistent the velocity of propagation is over the length of the cable. Typically this error is 3%–5%.

The global minimum found by the optimization was 81. This small discrepancy (expected 79) can be due to the delay introduced by the coupler, the improper synchronization of the test signal and the received signal while acquiring the data on the digital oscilloscope and/or the measurement (of the cable length), or error in the velocity of propagation.

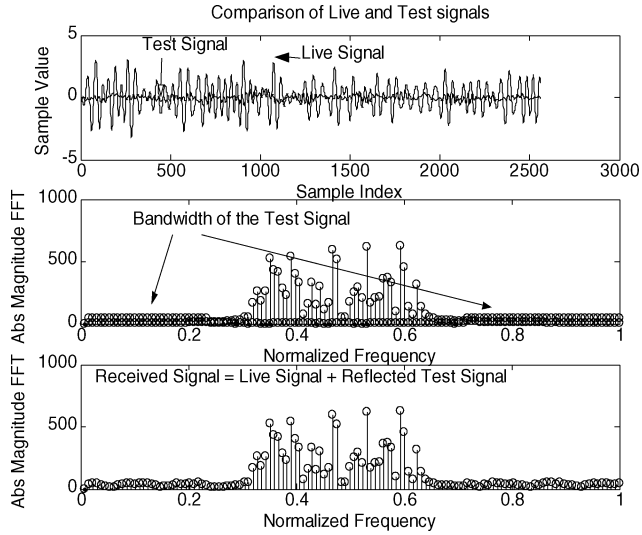

Fig. 10. Subplot 1: Time domain versions of live and test signal. Subplot2: FFT of live and test signal. Subplot 3: FFT of the received signal.

In order to locate intermittent faults that may be on the order of a few milliseonds, the system should first compare the raw data from successive periods of the test signal. When a change is detected, the optimization is applied to determine the distance to fault. In practical applications envisioned today, the fault detection and data acquisition is needed in real time, but the optimization used for calculation of distance to fault from this data can be done off-line when the fault is ready to be repaired. The optimization takes only a couple of seconds on a PC and is, therefore, highly suitable for directing maintenance actions.

VI. Live Wire Fault Detection

It is possible to use MCR for locating faults on live wires with a signal containing power (low frequency) or digital data (high frequency). If we assume that the live signal that already exists on the cable is band-limited, then we can avoid using this bandwidth while creating our test signal. The out-of-band noise exhibited by these live signals can be minimized using averaging as mentioned in Section II. Preliminary simulations done in this area show promising results. To simulate these conditions, white noise was passed through a band-pass filter to obtain a particular band-limitation between 950 kHz to 1 MHz. Then, the test signal, shown in Fig. 10, was carefully constructed to use frequencies below and above this bandwidth with amplitude well below the live signal (-15 dB down). It is clear that we have reduced the number of frequencies for the computations in the optimization algorithm. However, these frequencies are still sufficient to approximate the delay and, hence, location to fault accurately.

Fig. 10 shows the FFT plots of test signal, the band-limited signal as the live signal, and the reflected signal that was obtained by delaying and scaling the test signal to include two reflections and then adding the live signal to it. It is evident that by avoiding the bandwidth of the live signal, we can still approximate the time delay accurately as seen from Fig. 11. These results were obtained by using (12) and (13) as described in Section IV. In Fig. 11, $k = 2\tau_D$.

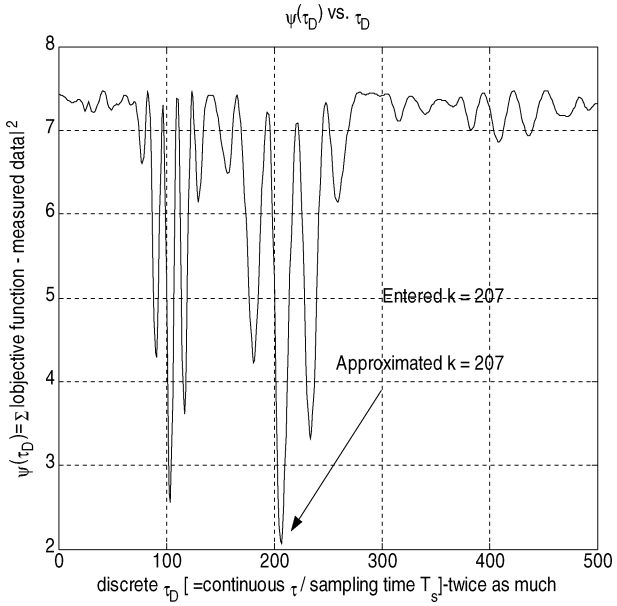

Fig. 11. Results of optimization on livewire signals.

VII. Conclusion

A new reflectometry method called MCR is proposed. In this method, a test signal is constructed by summing up sinusoids of the desired frequencies. This test signal is sent onto the cable and then the received signal is examined to retrieve information regarding the reflections from the cable. A frequency domain analysis is used in order to approximate the time delay exhibited by the cable reflections and, thus, the length of the cable the distance to the fault. The proposed MCR was tested in an experimental setup and shown to work effectively. Application of MCR to testing of live wires was also addressed, and its feasibility was demonstrated through simulations.

References

[1] National Transportation Safety Council (NTSC), Review of Federal Programs for Wire System Safety, White House Rep. Nov. 2000.
[2] M. Schmidt, "Use of TDR for cable testing" M.S. thesis, Dept. Elect. Comput. Eng., Utah State Univ., Logan, 2002 [Online]. Available: http://wwwlib.umi.com/dissertations/
[3] C. Furse *et al.*, "Frequency domain reflectometry for on board testing of aging aircraft wiring," *IEEE Trans. Electromagn. Compat.*, no. 2, pp. 306–315, May 2003.
[4] P. Tsai, Y. Chung, C. Lo, and C. Furse, "Mixed signal reflectometer hardware implementation for wire fault location," *IEEE Sensors J.*, vol. 5, no. 6, pp. 1479–1482, Dec. 2005.
[5] N. Amarnath, "Capacitance and inductance sensors for the location of faults in wires," M.S. thesis, Dept. Elect. Comput. Eng., Univ. Utah, Salt Lake City, 2004.
[6] P. Smith, C. Furse, and J. Gunther, "Fault location on aircraft wiring using spread spectrum time domain reflectometry," *IEEE Sensors J.*, vol. 5, no. 6, pp. 1469–1478, Dec. 2005.
[7] B. Farhang-Boroujey and T. Tay, "Transfer function identification with filter techniques," *IEEE Trans. Signal Process.*, vol. 44, no. 6, pp. 1334–1345, Jun. 1996.
[8] S. Naik, "Fault location in wires using multicarrier reflectometry," M.S. thesis, Dept. Elect. Comput. Eng., Univ. Utah, Salt Lake City, 2004.
[9] B. Farhang-Boroujeny, *Adaptive Filters*. Chichester, U.K.: Wiley, 1998.
[10] *"XtremeDSP Development Kit User's Guide"* [Online]. Available: http://www.nallatech.com.
[11] M. R. Shroeder, "Synthesis of low-peak-factor signalsand binary sequences with low autocorrelation," *IEEE Trans. Inf. Theory*, vol. 16, no. 1, pp. 85–89, Jan. 1970.
[12] A. Van den Bos, "A new method for synthesis of lowpeak-factor signals," *IEEE Trans. Acoust., Speech, Signal Process.*, vol. 35, no. 1, pp. 120–122, Jan. 1987.
[13] C. Lo and C. Furse, "Noise domain reflectometry for locating wiring faults," *IEEE Trans. Electromagn. Compat.*, vol. 47, no. 1, pp. 97–104, Feb. 2005.
[14] J. Proakis *et al.*, "Chapter 5: Least-squares methods for system modeling and filter design," in *Advanced Digital Signal Processing*, J. Proakis, Ed. *et al.* New York: Macmillan, 1992, pp. 256–262.
[15] L. Griffiths, R. Parakh, C. Furse, and B. Baker, "The invisible fray: A critical analysis of the use of reflectometry for fray location," *IEEE Sensors J.*, vol. 6, no. 3, pp. 697–706, Jun. 2006.
[16] C. Furse, P. Smith, M. Safavi, and C. Lo, "Feasibility of spread spectrum reflectometry for location of arcs on live wires," *IEEE Sensors J.*, vol. 5, no. 6, pp. 1445–1450, Dec. 2005.
[17] C. Lo, K. Nagoti, A. Mahoney, Y. C. Chung, and C. Furse, "Detection and mapping of branched wiring networks from reflectometry responses," presented at the Aging Aircraft Conf., Palm Springs, CA, Jan. 31–Feb. 4 2005.
[18] Y. Chung, N. Amarnath, C. Furse, and J. Mahoney, "Capacitance and inductance sensors for location of open and short circuited wires," *IEEE Trans Instrum. Meas.*, to be published.
[19] R. Parakh, "The invisible fray: A formal assessment of the ability of reflectometry to locate frays on aircraft wiring," M.S. thesis, Dept. Elect. Comput. Eng. Univ. Utah, Salt Lake City, 2004.

Suketu Naik received the B.S. degree in electrical engineering from Utah State University, Logan, in 2002, and the M.S. degree in electrical engineering from the University of Utah, Salt Lake City, in 2004.

He is currently with the Communiation and Information Systems Department, Spawar Systems Center, San Diego, CA. His interests include RF communications and digital signal processing.

Cynthia Furse (SM'99) received the Ph.D. degree in 1994.

She is the Director of the Center of Excellence for Smart Sensors, University of Utah, Salt Lake City, where she is also a Professor in the Electrical and Computer Engineering Department. The Center focuses on embedded sensors in complex environments, particularly sensors for anomalies in the human body and aging aircraft wiring. She has directed the Utah "Smart Wiring" program, sponsored by NAVAIR and USAF, since 1997. She teaches electromagnetics, wireless communication, computational electromagnetics, microwave engineering, and antenna design.

Dr. Furse was the 2000 Professor of the Year at the College of Engineering, Utah State University, Logan, the 2002 Faculty Employee of the Year, a National Science Foundation Computational and Information Sciences and Engineering Graduate Fellow, IEEE Microwave Theory and Techniques Graduate Fellow, and Presidents Scholar at the University of Utah. She is the Chair of the IEEE Antennas and Propagation Society Education Committee and an Associate Editor of the IEEE Transactions on Antennas and Propagation.

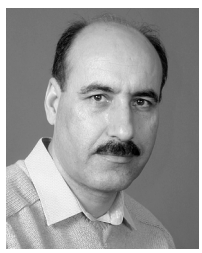

Behrouz Farhang-Boroujeny (M'84–SM'90) received the B.Sc. degree in electrical engineering from Teheran University, Tehran, Iran, in 1976, the M.Eng. degree from University of Wales Institute of Science and Technology, U.K., in 1977, and the Ph.D. degree from Imperial College, University of London, London, U.K., in 1981.

From 1981 to 1989, he was with the Isfahan University of Technology, Isfahan, Iran. From 1989 to 2000, he was with the National University of Singapore. Since August 2000, he has been with the University of Utah, Salt Lake City. He is an expert in the general area of signal processing. His current scientific interests are adaptive filters, multicarrier communications, detection techniques for space-time coded systems, and signal processing applications to optical devices. In the past, he has made significant contributions to the areas of adaptive filter theory, acoustic echo cancellation, magnetic/optical recodings, and digital subscriber line technologies. He is the author of the book *Adaptive Filters: theory and applications* (Wiley, 1998). He currently serves as associate editor of IEEE Transactions on Signal Processing.